

Materials and methods.

Western blot analysis

Protein lysates were extracted from PIPWF-treated and untreated (control) AsPC-1, CAFs and A549 cells, separated by 10% SDS-PAGE, and transferred to PVDF membranes. After blocking with 5% non-fat milk for 2 h at 25°C, the membranes were incubated overnight at 4°C with primary antibodies (1:1000 dilution) against Pin1, β -actin, CDK4, CDK6, CDK2, ERK, p-ERK, Akt, p-Akt, Kras, β -catenin, collagen, α -SMA, GAPDH, fibronectin, N-cadherin, E-cadherin, ENT1, FAP- α , vimentin and PPIA. Subsequently, the membranes were incubated with appropriate HRP-conjugated secondary antibodies (1: 2000 dilution) for 2 h at 25 °C. Protein bands were visualized using enhanced chemiluminescence (ECL) reagents (Pierce, USA).

Surface plasma resonance (SPR) analyses

A 1 mM stock solution of PIPWF peptide was serially diluted in ddH₂O to concentrations ranging from 1.56 nM to 200 nM. Aliquots (10 μ L) of each dilution were spotted onto gold sensor chips and incubated overnight at 4 °C in a humidified chamber. After incubation, chips were washed sequentially with 10 \times PBST, 1 \times PBST, and ddH₂O. Non-specific binding sites were blocked with 5% non-fat milk overnight at 4 °C, followed by identical washing steps. SPR measurements were performed on a PlexArray HT system (Plexera Bioscience) using a 660 nm collimated light source. Pin1 solutions in PBST were perfused through the flow cell at varying concentrations. Each measurement cycle consisted of: (i) 120 s baseline stabilization with PBST (2 μ L/s), (ii) 300 s sample injection (2 μ L/s), (iii) 300 s dissociation phase with PBST (2 μ L/s), and (iv) 300 s surface regeneration with 0.5% H₃PO₄ (2 μ L/s). All measurements were conducted at 20 °C, and the signal changes post-binding and washing were recorded. Binding kinetics were analyzed using the manufacturer's Data Analysis Module and BIA evaluation 4.1 software (Biacore).

Molecular dynamics (MD) simulation and binding free energy calculations

MD simulations were performed using GROMACS 2021 with the CHARMM36m force field to investigate three systems: Pin1-PIPWF, Pin1-AKT-pThr450, and Pin1-AKT-pThr450-PIPWF.^[1,2] The ternary complex structure was constructed by aligning the stable binding conformations of Pin1-PIPWF and Pin1-AKT-pThr450, with AKT phosphorylation at Thr450 modeled using CHARMM-GUI. All systems were solvated in a TIP3P water box and energy-minimized for 5,000~10,000 steps.^[3] After gradual heating from 0 K to 298 K, systems were equilibrated for 0.2 ns followed by 30 ns production runs in the NPT ensemble at 298 K. The SHAKE algorithm constrained hydrogen bonds,^[4] while Van der Waals (vdW) interactions were truncated at 1 nm and electrostatic interactions were calculated using the particle mesh Ewald (PME) with a 1 nm real-space cutoff. Simulations employed a 2.0 fs timestep with coordinates saved every 10 ps.

For the Pin1-AKT-pThr450 system, periodic annealing was performed through

three 2-ns cycles, each involving temperature reduction from 500 K to 298 K (1 ns) followed by equilibration at 298 K (1 ns). Hydrogen bond analysis during cooling phases identified stable conformations at the Thr450 phosphorylation site for further simulation. The system stability was assessed through root mean square deviation (RMSD) analysis of trajectories. The most stable conformations were subjected to binding free energy of association (ΔG) calculations using the MM/GBSA method with *gmx_MMPBSA*.^[5,6] MM/GBSA estimates the free energy difference between the bound and unbound states of solvated molecules through a thermodynamic cycle (Eq. 1).

$$\Delta G_{bind} = G_{complex} - G_{receptor} - G_{ligand} = \Delta E_{MM} + \Delta G_{GB} + \Delta G_{SA} - T\Delta S \quad (1)$$

In the Eq. (1), ΔE_{MM} represents the interaction energy between the receptor and ligand in the gas phase, including both electrostatic and van der Waals contributions. ΔG_{GB} and ΔG_{SA} correspond to the polar and nonpolar components of the solvation free energy, respectively. Interaction entropy (ΔS) was excluded from this study due to the significant computational cost of its calculation. The polar solvation energy (ΔG_{GB}) was computed using the GBOBC1 model as implemented in the *gmx_MMPBSA* tool,^[7] while the nonpolar solvation energy (ΔG_{SA}) was estimated based on the solvent-accessible surface area (SASA) using the Linear Combination of Pairwise Overlaps (LCPO) method.^[8]

Cell viability assay

Cell viability was assessed using the CCK-8 assay. AsPC-1 cells and CAFs were seeded in 96-well plates at 5×10^4 cells/well and allowed to adhere overnight. Cells were then treated with varying concentrations of PIPWF for 24, 48, or 72 h. After treatment, the medium was replaced with 10 μ L CCK-8 reagent per well and incubated for 2 h. Absorbance at 450 nm was measured using a SpectraMax i3 microplate reader (Molecular Devices), with PBS-treated cells serving as negative controls.

[illegible]

Figure S1. Molecular interactions between Pin1 protein and PIPWF peptide. (a) Binding energy diagram of amino acid interactions between PIPWF peptide and Pin1 protein. This diagram highlights the binding energies of the key amino acid residues involved in the interaction. (b) The hydrophobic interaction between *Leu123* in Pin1 and Trp13 in the PIPWF shows the most robust binding energy of -7.3 kcal/mol. (c) π - π interactions are observed between Trp1 of the PIPWF and *Arg120* of Pin1, as well as between Trp20 of the PIPWF and *Gln132* of Pin1. (d) Hydrogen bonding interactions are observed between several residues: Trp1 with *Lys118*, Gly12 with *Ser115*, Trp13 with *Met131*, Asp16 with *Ser155*, Asp19 with *Arg70*, Tyr2 with *Lys133*, and Lys23 with *Asp154*, respectively.

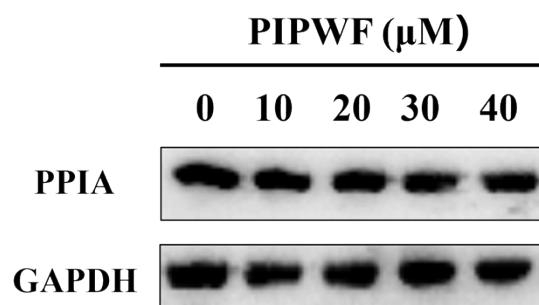


Figure S2. The protein expression levels of PPIA and GAPDH were analyzed by Western blot.

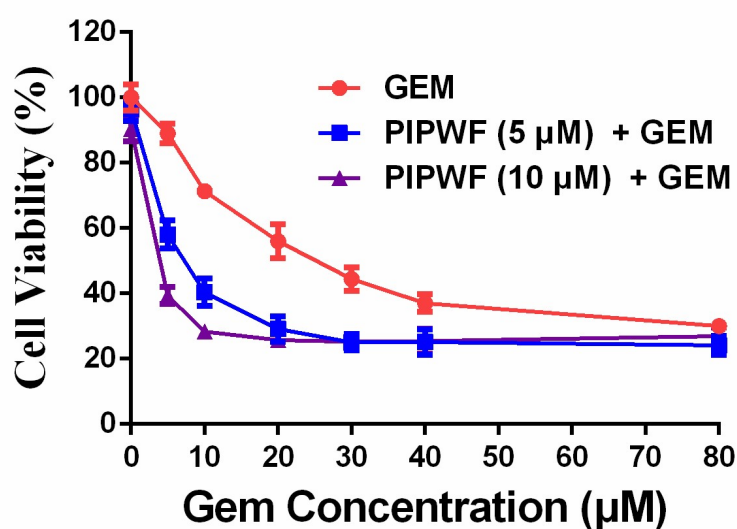


Figure S3. Cytotoxicity of Gemcitabine alone and in combination with PIPWF peptide in AsPC-1 cells. Cytotoxic effects were assessed using the CCK-8 assay after 48 h of incubation with varying concentrations of GEM alone (5 μM, 10 μM, 20 μM, 30 μM, 40 μM and 80 μM), or in combination with 5 μM or 10 μM PIPWF peptide. Data are presented as mean ± standard deviation from three independent experiments.

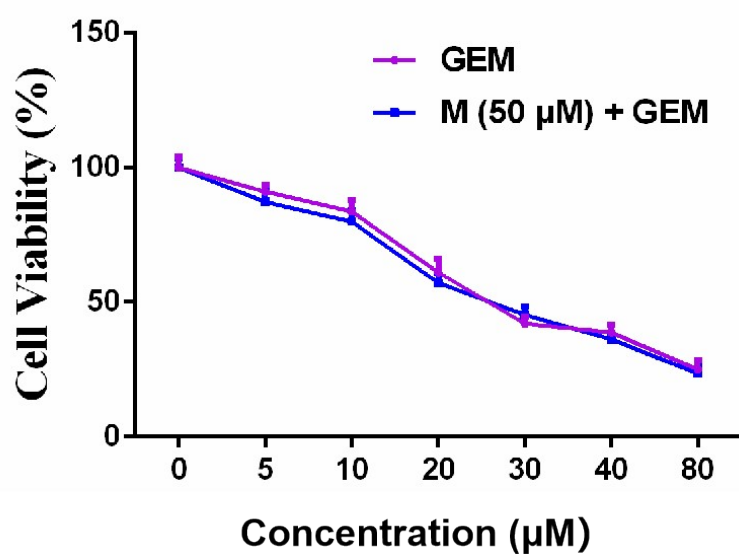
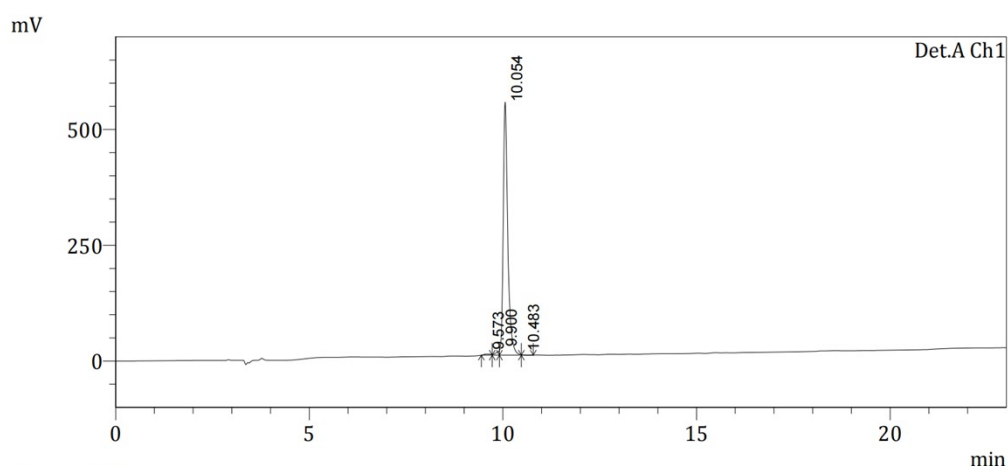


Figure S4. Cytotoxicity of GEM alone and in combination with 50 μ M PEG-PE micelles (M) in AsPC-1 cells. Cytotoxic effects were assessed using the CCK-8 assay after 48 h of incubation with varying concentrations of GEM (5 μ M, 10 μ M, 20 μ M, 30 μ M, and 40 μ M), or in combination with 50 μ M PEG-PE micelles. Data are presented as mean \pm standard deviation from three independent experiments.



1 Det.A Ch1/220nm

PeakTable

Detector A Ch1 220nm

Peak#	Ret. Time	Area	Height	Area %	Height %
1	9.573	32109	2583	0.707	0.463
2	9.900	56041	9023	1.233	1.616
3	10.054	4454213	546097	98.026	97.808
4	10.483	1525	633	0.034	0.113
Total		4543888	558336	100.000	100.000

Figure S5. High-Performance Liquid Chromatography (HPLC) analysis of the PIPWF peptide.

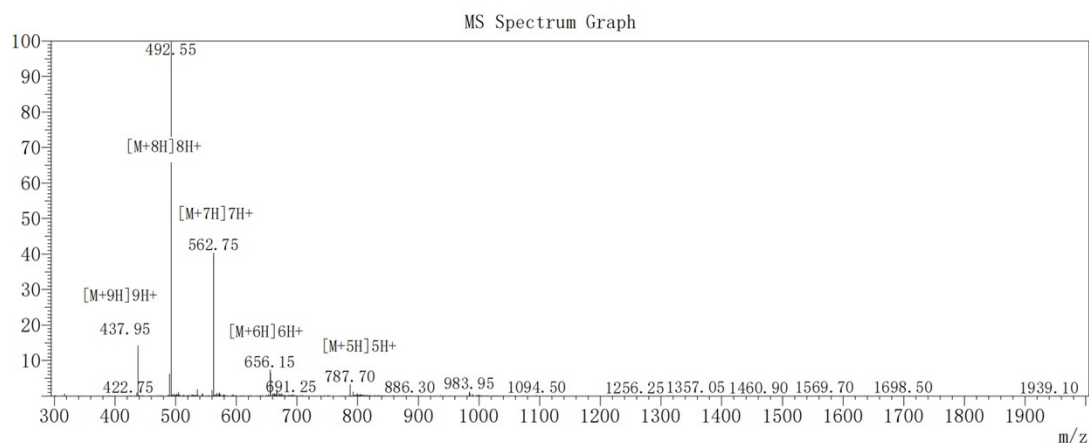


Figure S6. Mass spectrometry (MS) analysis of the PIPWF peptide.

Table S1. CD spectroscopy-derived secondary structure composition of Pin1 upon PIPWF interaction.

Molar ratios (PIPWF : Pin1)	α-helix (%)	β-sheet (%)	β-Turn (%)	Random-coil (%)	Total (%)
Pin1 (2 μ M)	17.30	55.00	4.30	23.40	100
0.2 : 1	16.30	51.30	6.70	25.70	100
0.3 : 1	13.03	55.87	4.27	26.87	100
0.4 : 1	13.23	50.90	6.03	29.80	100
0.5 : 1	10.83	54.57	5.23	29.40	100
1 : 1	7.90	54.90	5.33	31.83	100
2 : 1	5.80	57.53	3.63	33.10	100
3 : 1	5.03	56.90	4.40	33.67	100
4 : 1	1.40	61.23	1.80	35.53	100
5 : 1	0.00	61.30	1.77	36.93	100
10 : 1	0.00	57.03	4.37	38.57	100

References.

1. Abraham, M. J.; Murtola, T.; Schulz, R.; Páll, S.; Smith, J. C.; Hess, B.; Lindahl, E. GROMACS: high performance molecular simulations through multi-level parallelism from laptops to supercomputers. *SoftwareX* **2015**, *1-2*, 19–25.
2. Huang, J.; Rauscher, S.; Nawrocki, G.; Ran, T.; Feig, M.; de Groot, B. L.; Grubmüller, H.; MacKerell, A. D. CHARMM36m: an improved force field for folded and intrinsically disordered proteins. *Nat. Methods* **2017**, *14*, 71–73.
3. Gil Pineda, L. I.; Milko, L. N.; He, Y. Performance of CHARMM36m with modified water model in simulating intrinsically disordered proteins: a case study. *Biophys. Rep.* **2020**, *6*, 80–87.
4. Ryckaert, J. P.; Ciccotti, G.; Berendsen, H. J. C. Numerical integration of Cartesian equations of motion of a system with constraints: molecular dynamics of n-alkanes. *J. Comput. Phys.* **1977**, *23*, 327–341.
5. Valdés-Tresanco, M. S.; Valdés-Tresanco, M. E.; Valiente, P. A.; Moreno, E. gmx_MMPBSA: a new tool to perform end-state free energy calculations with GROMACS. *J. Chem. Theory Comput.* **2021**, *17*, 6281–6291.
6. Miller, B. R.; McGee, T. D.; Swails, J. M.; Homeyer, N.; Gohlke, H.; Roitberg, A. E. *MMPBSA.py*: an efficient program for end-state free energy calculations. *J. Chem. Theory Comput.* **2012**, *8*, 3314–3321.
7. Onufriev, A.; Bashford, D.; Case, D. A. Exploring protein native states and large-scale conformational changes with a modified generalized born model. *Proteins* **2004**, *55*, 383–394.
8. Weiser, J.; Shenkin, P. S.; Still, W. C. Approximate atomic surfaces from linear combinations of pairwise overlaps (LCPO). *J. Comput. Chem.* **1999**, *20*, 217–230.